The physical mechanism of operation of the Pirani vacuum sensor in the temperature stabilization mode

© E.V. Rut'kov,[1] O.A. Beliaeva,[2] N.A. Belik,[2] E.Yu. Afanas'eva,[1] D.B. Salin,[3] N.R. Gall[1]

[1]Ioffe Institute,
194021 St. Petersburg, Russia
[2]TECHNAN,
199155 St. Petersburg, Russia
[3]Modern Vacuum Systems
194223 St. Petersburg, Russia
e-mail: rutkov@ms.ioffe.ru

An experimental study of the processes on the surface of a metal heater (filament), which determine the physical mechanism of operation of a Pirani-type vacuum sensor in a wide pressure range of $1000-10^{-3}$ mbar for the main components of air: nitrogen and oxygen has been made. It is shown that in the mode of stabilization of the constant temperature of the heater, the mechanism of power removal by the gas from the surface changes significantly with a change in pressure. At $p = 10^{-3}-10^{-1}$ mbar, heat is carried away by molecules adsorbed on the surface over a layer of chemisorbed nitrogen or oxygen atoms. At high pressures, the molecular layer is almost completely filled, and additional heat removal is carried away by molecules adsorbing into the second (physisorbed) layer; in this case, the efficiency of heat removal sharply decreases, almost 1000 times per molecule.

Keywords: vacuum measurement, Pirani sensor, tungsten, nitrogen, molecular chemisorption, thermal desorption.

Introduction

Thermoelectric sensors, in particular the sensor proposed by M. Pirani at the beginning of the last century [1], remain the main means of measuring the level of the so-called „low" vacuum, i.e. pressures ranging from 1000 mbar (one atmosphere) to level $10^{-2}-10^{-3}$ mbar. An important scientific and technical problem, which is the subject of a large number of publications [2–9], is the desire to expand the measured range from low pressures. In fact, expanding this range by at least one order of magnitude, to the level of $10^{-3}-10^{-4}$ mbar, would make it possible to reliably connect a thermoelectric sensor with a high-vacuum magnetic-discharge sensor that uses the dependence of the ion discharge current on pressure. Today, the combination of these two sensors is the main combination for the vast majority of wide-range vacuum gauges

Recently, the efforts of many authors have been focused on the development of Pirani sensors based on modern thin-film systems using microelectromechanical systems (MEMS) technology [6]. From a physical point of view, this approach looks promising, since it allows one to achieve a high ratio of the heater surface to its volume. At the same time, traditional heaters made of thin wire retain their importance, since they are technologically simple and reliable. Moreover, the physical processes that determine the operation of the sensor are the same regardless of the type of heater.

One of the scientific problems standing in the way of solving the problem posed above is the lack of a clear molecular physical mechanism that allows to prefer one or another type of thermoelectric sensor heater operation. It has been empirically established that the operating mode associated with stabilizing the resistance of the wire heater, and therefore its temperature, is preferable. But what is its physical cause? In itself, consideration of thermal processes in the sensor based on the models presented in [10] and [2] does not allow us to draw such conclusions.

Physical processes occurring on the surface of a wire heater in a Pirani sensor in a wide range of gas pressures were studied in our work [11]. A molybdenum filament with a diameter of 150μm was used as a heating element and nitrogen or air as a gas. In this work, a physical molecular mechanism was developed that makes it possible to qualitatively explain the well-known Z-shaped curves of the dependence of the heater resistance on gas pressure. However, the mechanisms influencing the type of operation of the sensor were not considered.

This work is devoted to the consideration of the physical mechanism underlying the operation of a Pirani-type sensor, as applied to methods for stabilizing temperature or current during heater operation.

1. Procedure and methods of experiment

The main experiments were carried out on a commercial sensor of the Pirani Technan NV 2 type, which used a

heater made of tungsten wire with a diameter of $100\,\mu$m in the form of a spiral with a diameter of 8 mm and a length of 100 mm, freely located on molybdenum holders. Tungsten is a technically accessible material with good electrophysical parameters and technological reproducibility. For experiments to the sensor, laboratory power supplies were connected, which made it possible not to rely on the operating modes embedded in the program of its controller.

Some of the experiments were carried out in a high-resolution ultra-high-vacuum ($p \leq 1 \cdot 10{-}10$ Torr). Auger spectrometer ($\Delta E/E \leq 0.1\%$) with a prism energy analyzer [12]. Although the adsorption properties of molybdenum and tungsten are close, there are also significant differences [13,14], therefore it seemed necessary to study the real regularities of adsorption and desorption of atmospheric gases on the surface of tungsten for comparison with the results of the work [11].

W- and Mo-samples in the form of thin ribbons of size $40 \times 1 \times 0.02$ mm were purified by heating to high temperatures of 1800 K in an oxygen atmosphere at $p_{O2} \sim 1 \cdot 10^{-5}$ Torr and then in ultra-high vacuum at $T = 2200$ K. After cleaning, only Auger peaks of tungsten or molybdenum, respectively, were observed on the surface. The sample temperature at $T > 900$ K was measured with an optical micropyrometer, and at $T < 900$ K using quadratic extrapolation of the temperature dependence on the sample heating current The temperature heterogeneity along the sample was less than 10 K over length of 40 mm. Nitrogen, oxygen and atmospheric air were used as the gas medium. When heated, the ribbons were textured, and the (100)W and (100)Mo faces appeared on the surface, which corresponded to the measured work functions $e\varphi_W = 4.65$ eV and $e\varphi_{Mo} = 4.45$ eV [15].

As the second experimental bench-unit, a vacuum laboratory stand was used, pumped out by an oil-free spiral fore pump, followed by pumping to a high vacuum$\sim 10^{-7}$ mbar using a turbomolecular pump. The W-wires and ribbons were resistively heated by direct current. The bench-unit had a needle leak, which allowed smoothly change of the nitrogen pressure in the chamber, and a port for a gas cylinder connection.

The temperature of the tungsten filaments in the sensor for the entire pressure range was determined using the well-known formula $R_t = R_0(1 + \alpha t)$, where the coefficient α was considered constant, $\alpha = 4.7 \cdot 10^{-3}\,^\circ C^{-1}$ [16]. In the region of pyrometric temperatures in high vacuum, a micropyrometer was additionally used. Note that good agreement was obtained with the temperature determined by the above-mentioned method. To accurately determine the resistance of the molybdenum filament a four-wire system was used, when the filament supply was „decoupled" and the voltage drop across it was measured.

2. Results and discussion

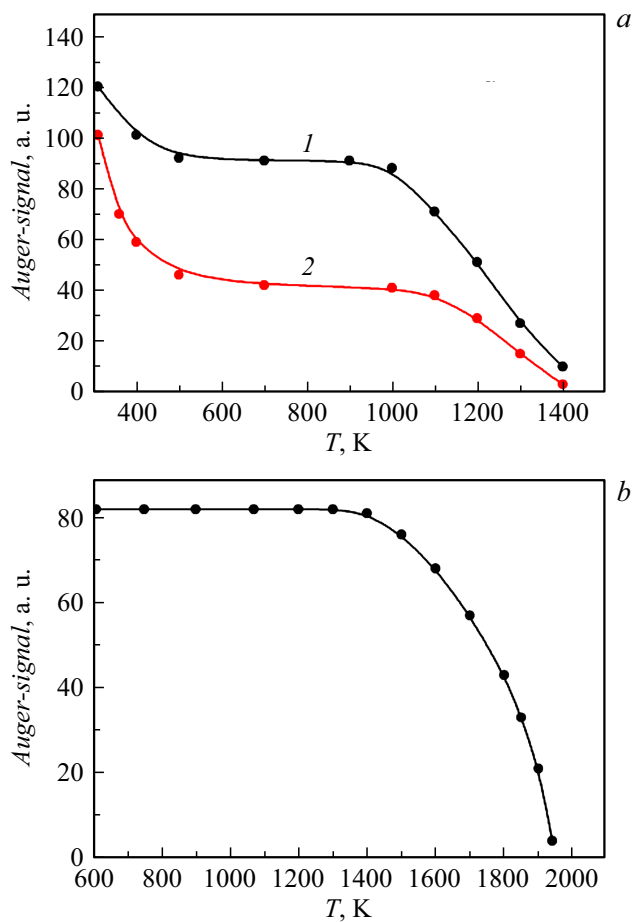To carry out the experiments, nitrogen with a purity of 10^{-6} was filled into the Auger spectrometer to a pressure

Figure 1. *a* — Variations in the Auger-signal of nitrogen on the W(100) (*1*) and Mo(100) (*2*) vs annealing temperature. Nitrogen adsorption at 300 K until saturation; *b* — dependence of the intensity of the Auger signal of oxygen on W(100) on the annealing temperature after adsorption of O_2 at 600 K. Waiting time at each point is 20 s.

of $1 \cdot 10^{-5}$ Torr at a temperature of tungsten and molybdenum ribbons of 300 K for 100 s, which approximately corresponds to an adsorption dose of the order of 3000 L. In this case, saturation is achieved on the surface: the Auger signals of nitrogen ($E = 379$ eV), tungsten ($E = 179$ eV) and molybdenum ($E = 221$ eV(remained constant and did not change with further exposure to nitrogen. After that, nitrogen was pumped out, and the dependence of both Auger signals on ribbon temperature was measured.

Fig. 1, *a* shows the dependence of the Auger signal of nitrogen upon annealing of tungsten 1 and molybdenum 2 ribbons. It can be seen that even a very slight heating, up to $\sim 400{-}500$ K, leads to the removal of part of the nitrogen from the surface: the intensity of the nitrogen Auger signal decreases, which indicates the desorption of part of the nitrogen from the surface. In this case, a noticeable thermally stable coating remains on both the (100)W and (100)Mo surfaces, which does not change up to $T = 1000{-}1100$ K. With further heating, nitrogen is

thermally desorbed and at $T > 1400$ K the surfaces of both tungsten and molybdenum are free of adsorbed gas.

The interaction of nitrogen with refractory metals has been studied in many works, for example, in [17]. Based on these works, it can be argued that in the region $500-1100$ K a layer of atomic chemisorbed nitrogen remains on the surface, which does not participate in adsorption-desorption equilibrium at low temperatures. From the literature data [17] and from Fig. 1, a (desorption temperature $T > 1100$ K) it follows that for this state the bond energy of nitrogen atoms with the metal (W, Mo) $\sim 3-4$ eV.

Another gas, the oxygen, which ranks two in concentration in atmospheric air ($\sim 21\%$) after nitrogen ($\sim 78\%$) behaves similarly.

Fig. 1, b shows the dependence of the intensity of the oxygen Auger signal ($E = 510$ eV) after the adsorption of O_2 at 600 K on (100)W. It is known from the literature that a layer of chemisorbed oxygen atoms with a concentration close to the concentration of surface tungsten atoms $1 \cdot 10^{15}$ cm^{-2} [14] is formed on the W(100) surface. As in the case of nitrogen, this coating is stable over a wide temperature range, and complete removal of oxygen occurs only at $T > 2100$ K. It is clear that in both the case of nitrogen and oxygen there is a concentration dependence of the bond energy of adatoms on the substrate, but in any case, this chemisorbed state corresponds to significant binding energies $\sim 4-5$ eV, i.e. chemisorbed atoms of oxygen, as well as nitrogen, have significant binding energy with the surface and will not participate in heat exchange between metal filament (ribbon) and gas environment at operating mode temperatures of the Pirani sensor $T < 600$ K.

It is obvious that when the temperature decreases ($T < 600$ K) or the gas pressure in the chamber increases, all strongly bound centers must be occupied by nitrogen or oxygen atoms. The probable location of the chemisorbed atom are „positions" between four metal atoms. Therefore, molecular adsorption will be observed then. Indeed, for example, as shown in the work [11], the bond energy for nitrogen with molybdenum after the formation of a chemisorbed layer decreases to ~ 0.5 eV. If the concentration N of strongly bound centers, for example, for oxygen on W(100) $N \sim 1 \cdot 10^{15}$ cm^{-2}, then the estimated concentration of weakly bound centers is probably close to the value of $10^{14}-10^{15}$ cm^{-2}, since the open area of the metal after the atoms occupy the strongly bound centers is still large and amounts to $\sim 50\%$.

Let us consider the experiments carried out in the second experimental unit and characterizing to a greater extent the technical side of the operation of the Pirani sensor.

Fig. 2 shows change in temperature of a tungsten filament with a diameter of 100μm and a length of 100 mm vs the filament current for two cases: in a vacuum $p < 10^{-3}$ mbar I and in a nitrogen atmosphere $p = 1000$ mbar 2. It can be seen that nitrogen at atmospheric pressure greatly reduces the temperature of the filament: for example, for $I = 450$ mA the temperature decreases from 900 (vacuum)
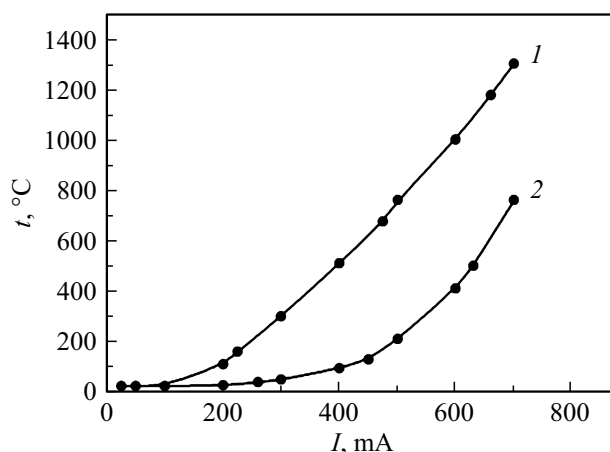

Figure 2. Dependence of the W filament temperature on the filament current: I — in vacuum ($p < 10^{-3}$ mbar); 2 — in a nitrogen atmosphere ($p \approx 1000$ mbar).
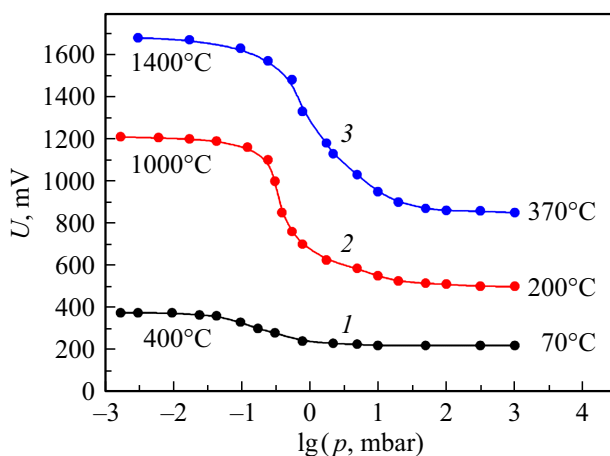

Figure 3. Dependence of the voltage at the W filament on $\lg p$ nitrogen for different filament currents: I — 300, 2 — 450, 3 — 550 mA.

to 150°C. This is a well-known effect, which is confirmed on all the materials we used.

Obviously, the filament resistance and its temperature will depend significantly on the nitrogen pressure in the chamber.

Fig. 3 shows the change in voltage at the tungsten filament vs the nitrogen pressure in the chamber for different filament currents (different power consumption $P = IU = I^2R$) and this is the traditional way of operating a Pirani-type sensor, when the voltage on the filament is related to the gas pressure in the chamber at $I =$ const.

As in our previous work [11], when using molybdenum filaments at a gas pressure of $p < 10^{-2}$ mbar, there is almost no change in the voltage at the filament with a change in pressure. It is obvious that under these conditions a small flux of gas molecules to the surface is not able to cool the filament [11]. The main events occur at nitrogen pressure $10^{-2} - 10$ mbar. At $p > 10$ mbar, a weak dependence of

Table 1. The lower limit for the sensitivity of the sensor for pressure (p) of the gas in the chamber depending on the power released on filament $P = IU$

$P = IU$, W	3.1	1.6	0.9	0.17	0.11	0.05	0.012
p, mbar	0.7	0.1	$6 \cdot 10^{-2}$	$3 \cdot 10^{-2}$	$1 \cdot 10^{-2}$	$3 \cdot 10^{-3}$	$2 \cdot 10^{-3}$

Figure 4. Dependence of the power released at the tungsten filament, $P = UI$ on $\lg p$: *1* — for the case of $I = \text{const} = 0.45\,\text{A}$; *2* — for the case of $R = \text{const}$ ($T = \text{const} = 200°\text{C}$).

the voltage at the filament on the gas pressure in the chamber is observed. „Heat removal" from the filament in this case is determined not by the gas flux from the outside, but by the lifetime of nitrogen molecules on the surface in a weakly bound state [11]. In other words, all places on the surface for nitrogen molecules under these conditions are already occupied and an increase in pressure (the flux of molecules to the surface) does not increase the heat exchange between the filament and the gas, i.e. the efficiency of the device decreases. In principle, it is possible to increase the efficiency of the sensor in the range of $10-1000$ mbar, increasing the power released on the filament, i.e. increasing its temperature and reducing the lifetime of nitrogen molecules on the surface, but this is catastrophic for the lifetime (operation) of a sensor using molybdenum or tungsten filaments at such high pressures and temperatures ($T > 1000°\text{C}$).

On the other hand, an increase in the power released at the filaments worsens the sensitivity of the sensor at low pressures.

Table 1 shows the power released on the tungsten filament, $P = IU$, and the lower limit of the „sensitivity" of the sensor for nitrogen pressure in the chamber, when the power released on the filament due to heat exchange with gas decreases by $3-5\%$. For example, if $P = 1.6\,\text{W}$, then the pressure at which the $p \geq 0.1\,\text{mbar}$ sensor begins to operate; if $P = 0.012\,\text{W}$, then $p \geq 2 \cdot 10^{-3}\,\text{mbar}$. Obviously, for practical use it is necessary to find the optimal operating mode of the sensor in order to minimize the above disadvantages.

Fig. 4 shows two graphs of the dependence of the power P released at the tungsten filament on $\lg p(N_2)$ in the chamber. Curve *1* corresponds to the traditional way of operation of the sensor, when $I = \text{const} = 450\,\text{mA}$ (curve *2* in Fig. 3). In this case, the temperature varies from 1000 to 200°C, which is unacceptable for tungsten for reasons of stability of the heater. The curve *2* was taken in the mode when $T = \text{const} = 200°\text{C}$ ($R = \text{const}$). In this case, both current I and voltage U are variable.

The problem of keeping up the electrical resistance $R = \text{const}$, and accordingly $T = \text{const}$, when gas pressure changes, is quite technically solvable. Traditionally, the Pirani sensor heater is included in one of the arms of the Winston bridge; when the pressure changes, the bridge becomes unbalanced due to an increase or decrease in temperature of the heater, and therefore its resistance. This imbalance is compensated by a corresponding increase or
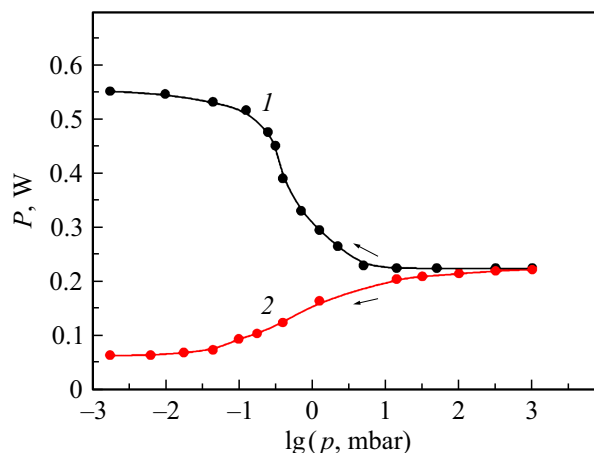
decrease in the filament current through the servo system so that the bridge always remains balanced. In this case, the filament current and voltage at the heater are used as a measured electrical signal, uniquely related to the pressure value.

For state-of-the-art, temperature constancy is easier to stabilize by digital method. To do this, simultaneous measurement of the current flowing through the heater and the voltage dropped across it is carried out; these values are digitized, the microprocessor calculates their ratio, which is proportional to the resistance of the heater filament, and therefore to the temperature. The tracking mode for stabilizing this ratio is implemented by microprogram, and the power dissipated by the heater is used as the output electrical signal.

The curve *2* in Fig. 4, obtained in this mode, turned out to be smoother with respect to the dependence on pressure and demonstrates greater contrast both in the region of high pressures $10-1000$ mbar and in the region of extremely low pressures, allowing one to confidently reach a value of the order of $2 \cdot 10^{-3}$ mbar. Note that when replacing the gaseous medium from nitrogen to atmospheric air, no differences were found in the results obtained. This is not surprising, since the composition of air mainly includes nitrogen (78%) and oxygen (21%), which is close to nitrogen in its adsorption properties in heat exchange mode. The remaining small impurities of other gases, apparently, cannot change the overall physical picture in the metal — gas heat exchange processes.

It's interesting that, the power versus pressure curve obtained in constant temperature mode also has a Z-shape, although inverted compared to the curve obtained in current stabilization mode. In the experiment, the pressure changed by 6 orders of magnitude, and the flux of gas molecules falling onto the surface changed by the same number of times, which directly follows from the Hertz-Knudsen formula [14]. However, the power dissipated by the heater,

Table 2. Gas flux density ν [s^{-1}] onto sensor filament, power P [W] removed by the gas, and average energy $< E >$ [J] carried off by one gas molecule per 1 s depending on the pressure in the chamber p [mbar]

p, mbar	ν, s^{-1}	P, W	$< E >= P/\nu$, J	P_0, W
1000	$8.8 \cdot 10^{22}$	0.173	$2.0 \cdot 10^{-24}$	570
100	$8.8 \cdot 10^{21}$	0.163	$1.9 \cdot 10^{-23}$	57
10	$8.8 \cdot 10^{22}$	0.145	$1.7 \cdot 10^{-22}$	5.7
1	$8.8 \cdot 10^{19}$	0.08	$1.1 \cdot 10^{-21}$	0.57
10^{-1}	$8.8 \cdot 10^{18}$	0.035	$4.8 \cdot 10^{-21}$	0.057
10^{-2}	$8.8 \cdot 10^{17}$	0.005	$5.7 \cdot 10^{-21}$	0.0057

*Note**: P_0 is calculated energy that would be carried away by all incoming molecules in 1 s for the hypothetical case when each molecule carries away the same portion of energy equal to kT: $P_0 = \nu\, kT$, where $T = 200°C = 473$ K.

and therefore the power removed by the gas, changed by only 3.2 times!

In order to use these data to discuss the molecular mechanism, it is necessary to take into account the role of other channels of heat loss from the heater that are not associated with heat removal by the gas. There are two such channels: thermal conductivity along the wire and thermal electromagnetic radiation. It is clear from the results of Fig. 4 that the heating power required to maintain a constant temperature of the heater ceases to depend on the gas pressure at $p < 10^{-3}$ mbar, i.e. the gas no longer makes a significant contribution to heat removal from the filament. Since the thermal conduction losses of the filament are very small, it can be assume that power is removed only by radiation at the operating temperature of the filament $T = 473$ K. Experimentally, this power is $P_r = 0.065$ W; the measured value agrees well with the calculation according to the Stefan-Boltzmann law under the assumption that in this wavelength region the emissivity is close to unity, which is usually true for the IR region [18]. Thus, all the remaining power released on the heater, minus $P_r = 0.065$ W, is removed by gas molecules.

Table 2, taking into account the above, presents the power P removed by gas, depending on the gas pressure in the chamber. The average energy P/ν per one gas molecule is also given for the case of their equally probable participation in heat removal from the filament.

In the work [11] we showed that the operation of the sensor in the pressure range close to atmospheric one is determined by the desorption of physically-adsorbed molecules from its surface, which do not have time to completely thermalize and carry off energy during desorption that is much less than kT. In this case, the experimentally observed contrast of the curve is determined by the dependence of the binding energy of the molecule adsorbed on the surface on the coverage, which in turn
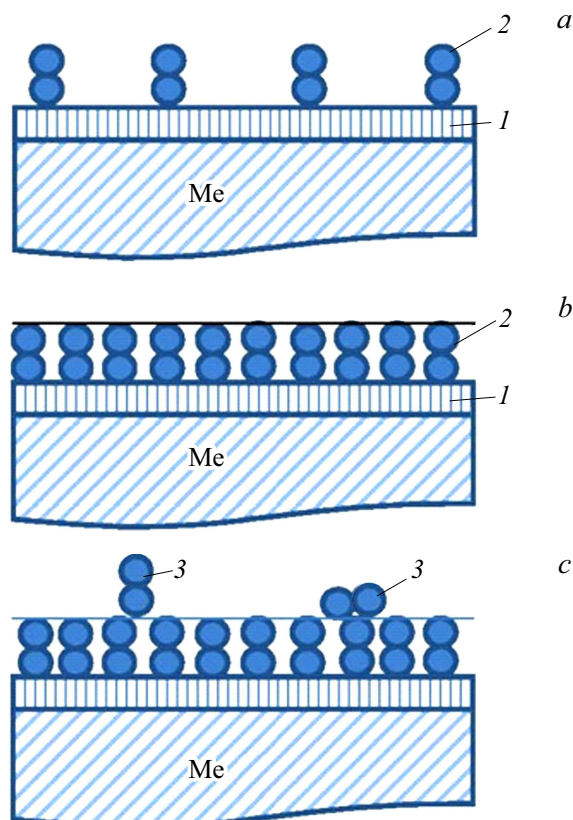

Figure 5. A simplified illustration of the processes of gas contact with a metal surface: *1* — chemisorbed layer of nitrogen atoms; *2* — chemisorbed molecules N_2 from the first layer with desorption energy ~ 0.5 eV; *3* — physically-adsorbed N_2 molecules from the second layer with extremely low desorption energy.

depends on the magnitude of the particle flux incident on the surface. In our opinion, the mechanism remains similar for the mode of thermostatic control: the surface of the heater over the entire pressure range $10^3 - 10^{-3}$ mbar is covered with a layer of chemisorbed atoms that do not take part in heat removal, and the entire „game" is determined by the molecules adsorbed on top of this layer. Simplified illustration of the process is shown in Fig. 5.

When discussing physical processes, first of all, it should be noted that at all pressures there is adsorption-desorption equilibrium on the surface, i.e. the flux of molecules falling from the gas ν is equal to the desorbed flux ν_{des}; Moreover, in the pressure range $2 \cdot 10^{-3} - 1000$ mbar, the flux of molecules ν incident on the surface changes by a factor of 500,000. As mentioned above, for the case of $p < 2 \cdot 10^{-3}$ mbar, the power released at the sensor does not depend on pressure; apparently this means that the flux of molecules is small and heat is removed from the filament only by radiation P_r, i.e. value P_0 is too small ($P_0 \ll P_r$). At $p \sim 10^{-1}$ mbar, the contribution of falling molecules to heat removal is already significant and the calculated value P_0 is close to the experimental value P,

i.e. all incidence molecules are thermalized and, during desorption, carry away energy close to kT.

Apparently this indicates that in this adsorption layer there is still no competition between molecules for places on the surface (Fig. 5, a). In fact, the concentration of molecules in the adsorption layer N is determined by the Langmuir relation for adsorption-desorption equilibrium $N = \nu\tau(1-\theta)$, where τ is the average lifetime of a molecule on the surface, determined by its binding energy and temperature, and θ is adsorbed molecules coverage, $\theta = N/N_\mathrm{m}$, where N_m is concentration of molecules in the monolayer. In our work [11], we determined the binding energy of such a chemisorbed molecule N_2 with the surface, assuming the first order of desorption in the layer; it was 0.5 eV, which coincides very well with the data presented here.

At higher pressures $p \approx 10^{-1}-10$ mbar, the picture changes sharply: molecules falling on the surface and desorbed from it carry away on average significantly less energy, i.e. $<E> \ll \mathrm{k}T$. The fact is that at these pressures the flux of molecules to the surface from the gas phase ν sharply increases and all adsorption sites in this layer turn out to be occupied by molecules N_2, $\theta \sim 1$ (Fig. 5, b). Since the surface temperature is constant, the desorption flux ν_des from this layer is now practically independent of pressure, and therefore the heat removal by molecules desorbed from the first layer is also independent of pressure. In fact, the power P removed by the molecules in this case is determined by the obvious formula: $P = <E> \nu_\mathrm{des} = <E> N_\mathrm{m}/\tau$

In the pressure range $10-1000$ mbar, the flux of molecules falling on the surface increases another 100 times, and the power removed from it increases only from 145 to 173 mW, i.e. only 1.2 times. If at $p = 1000$ mbar all the molecules desorbed from the surface would carry away the same average energy $<E> = \mathrm{k}T$, then the gas could remove very great power from the filament $P_0 = 570$ W, which is not observed in the experiment.

Apparently, in this pressure range, additional heat removal is carried out by molecules adsorbed onto the surface into a second layer on top of the chemisorbed molecular layer (Fig. 5, c). Physically-adsorbed molecules from this layer have very low binding energies with the surface, and apparently do not thermalize, carrying away very small portions of energy during desorption. Note that direct observation of a layer of physically-adsorbed molecules is practically impossible using modern rather hard research methods, such as electron spectroscopy, low-energy electron diffraction, etc. However, these experiments make it possible to judge it indirectly by the power removed by the molecules. Apparently these molecules have very low bond energies of the order of $< 10^{-1}$ eV and, accordingly, a very short lifetime on the surface, which is consistent with the data presented in [19].

Conclusion

Thus, the molecular mechanism that describes the removal of heat from the heater in a Pirani-type vacuum sensor, proposed in our work [11], is quite suitable for describing its operating mode under conditions of maintaining a low constant temperature. It can be expected that switching to a heater material that has a lower ability to bind molecules on a surface can increase the contrast of the sensor operation both in the high pressure region and, more importantly, in the extremely low pressure region.

Conflict of interest

The authors declare that they have no conflict of interest.

References

[1] M.S. Pirani. Dtsch. Phys. Ges. Verh., **8**, 686 (1906).

[2] S. Borichevsky. *Understanding Modern Vacuum Technology* (CreateSpace Independent Publishing Platform, 2017), p. 62. ISBN 9781974554461

[3] S. Chen, L. Feng, S. Guo S, Y. Ji, S. Zeng, X. Peng, Y. Xu, T. Hu, Z. Wu, S. Wang. Sensors, **23**, 1276 (2023). https://doi.org/10.3390/s23031276

[4] L. Zhang, J. Lu, H. Takagi, S. Matsumoto, E. Higurashi. Micromachines, **13**, 1686 (2022). https://doi.org/10.3390/mi13101686

[5] K.G. Punchihewa, E. Zaker, R. Kuljic, K. Banerjee, T. Dankovic, A. Feinerman, H. Busta. Sensors, **12**, 8770 (2012). DOI: 10.3390/s120708770

[6] S. Xu, N. Zhou, M. Shi, C. Zhang, D. Chen, H. Mao. Micromachines, **13**, 945 (2022). https://doi.org/10.3390/mi13060945

[7] W. Jitschin, S. Ludwig. Vakuum in Forschung und Praxis, **16** (1), 23 (2004). DOI:10.1002/vipr.200400015

[8] E.S. Topalli, K. Topalli, S.E. Alper, T. Serin, T. Akin. IEEE Sensors J., **9** (3), 263 (2009). DOI: 10.1109/JSEN.2008.2012200

[9] J. Chae, J.M. Giachino, K.J. Najafi. Microelectromech. Syst., **17** (1), 193 (2008). DOI: 10.1109/JMEMS.2007.910258

[10] A.K. Kikoin, I.K. Kikoin. *Molecular Physics* (Nauka, Moscow, 1976) (in Russian)

[11] E.V. Rut'kov, O.A. Beliaeva, N.R. Gall. Tech. Phys., **68** (2), 267 (2023). DOI: https://doi.org/10.21883/TP.2023.02.55483.187-22

[12] N.R. Gall, E.V. Rut'kov, A.Y. Tontegode. Tech. Phys., **47** (4), 484 (2002). DOI: http://dx.doi.org/10.1134/1.1470600

[13] M. Roberts, Ch. Makki. *Khimiya poverkhnosti razdela metall–gaz* (Mir, M., 1981) (in Russian)

[14] E. Bauer, H. Poppa, Y. Viswanath. Surf. Sci., **58**, 517 (1976).

[15] V.S. Fomenko. *Emissionnye svojstva materialov* (Kiev, Nauk. dumka, 1981)(in Russian)

[16] *Tables of physical quantities*, reference book ed. acad. I.K. Kikoin (Atomizdat, M., 1976) (in Russian)

[17] I. Tovoshima, G.A. Somorjai. Catalys. Rev. Sci. Engineer., **19** (1), 105 (1979). https://doi.org/10.1080/03602457908065102

[18] L. Michalski, K. Eckersdorf, J. Kucharski, J. McGhee. *Temperature Measurement* (John Wiley & Sons, Chichester, 2001), p. 162−208. ISBN 978-0-471-86779-1

[19] J. Condon. *Surface Area and Porosity Determinations by Physisorption, 2nd edition. Measurement, Classical Theory and Quantum Theory* (Elsevier, Amsterdam, 2020), p.93−215.

Translated by V.Prokhorov